論文 94-5-3-4

이동 위성 통신 채널에서 다이버시티 수신기법을 적용한 BPSK 및 QPSK 신호의 오율 특성

Error Performance of BPSK and QPSK Signals with Diversity Reception in Mobile-Satellite Communication Channel

박 해 천* · 강 영 흥** · 황 인 관*** · 조 성 준****

(Hae Cheon Park* · Young Heung Kang** · In Kwan Hwang*** · Sung Joon Cho****)

요 약

업링크와 다운링크 경로상에 각각 가산성 백색 가우스잡음이 존재하는 이동 위성 통신로에서 TWTA의 비선형성에 의한 BPSK신호와 QPSK신호의 오율성능을 조사하였다. 다운링크 경로상의 페이딩은 Rician 분포를 한다고 가정하였다. 또한 선택적 다이버시티에 대한 효과를 분석하였다. 선택적 다이버시티의 확률밀도함수에 관한 N차 모멘트를 구하였으며, 선택적 다이버시티의 확률밀도함수에 대한 근사 이산 확률분포를 고전적인 모멘트 기법 (CMT)을 이용하여 유도하였다. 오율은 Gauss Quadrature Formula와 근사 이산 확률 분포를 이용하여 계산하였다.

Abstract

The error performance of BPSK and QPSK signals with diversity reception in mobile-satellite channel is investigated considering nonlinearity of TWT (Traveling Wave Tube) amplifier in the presence of AWGN (Additive White Gaussian Noise) on the uplink and downlink paths. It is assumed that the fading on the downlink path forms a Rician distribution.

The Rician distribution is approximated by discrete probability values. The values are firstly found by Classical Moment Technique.

* 한국항공대학교 대학원 항공전자공학과(Dept. of Avionics Eng. Graduate School, Hankuk Aviation University)

** 군산대학교 공과대학 정보통신공학과(Dept. of Infor. and Telecomm. Eng., Kunsan National University)

*** 한국전자통신연구소(Electronics and Telecommunications Research Institute)

**** 한국항공대학교 항공통신정보공학과(Dept. of Telecomm. and Infor. Eng., Hankuk Aviation University)

Ⅰ. Introduction

The major difference between mobile-satellite communication and terrestrial mobile communication is in path loss, noise environment, and fading characteristics[1]. That is, in the analysis of mobile-satellite communication channel, not only an analysis for the environment of the fixed satellite communication channel but also an analysis for the mobile environment should be considered.

The objective of this paper is to investigate the error performances of BPSK (Binary Phase Shift Keying) & QPSK (Quaternary Phase Shift Keying) signals transmitted in the mobile-satellite channel considering nonlinearity of TWT amplifier in the presence of AWGN (Additive White Gaussian Noise) on the uplink and downlink paths and the degree that the diversity schemes can bring the error performance up in said system environment.

For mobile-satellite communication, the channels can be modeled in most cases as non-frequency selective Rician channels for which the fading amplitude obeys a Rician distribution. It is known that fading degrades the performance of communication systems. The fade margin for BPSK and QPSK systems on channel impaired by Rician fading has been examined, and some error performances considering just the path loss on the downlink and Rician channel had been derived[2].

For the fixed satellite communication, however, the error performances considering the path losses on the uplink and downlink had been analyzed, and it had been proven through such analyses that the uplink noise parameter has a serious effect on the system performance[3, 4, 5].

Therefore, in mobile-satellite communication, the analysis of the error performance considering the uplink noise parameter in addition to the conventional analyses is required in order that it may be used as a method for the design of the system to reduce the degradation of such system.

Accordingly, this paper provides the overall performance analysis considering the physical environments, that is, the path losses on the uplink and downlink, nonlinear TWT (Travelling Wave Tube) amplifier, Rician channel, and finally the diversity reception for improving the error performance.

The overall performance is obtained by using the discrete value for the Rician pdf firstly obtained in this paper by applying the Classical Moment Technique that is more accurate than Gauss Quadrature Formula being generally used to solve complex performance function.

Ⅱ. System Model

A bandlimited nonlinear mobile-satellite communication system is modelled as shown in [Fig. 1] in which the effect of fading and diversity reception is considered in the downlink path with AWGN in the uplink and the downlink paths. We also assume that the bandwidth of the downlink filter in wide enough to pass the transponder output without significant distortion.

Let us consider the PSK signal sequence to be modeled as

$$m(t) = \sqrt{2P}\sum_{k} p(t-kT)\cos(\omega_c t + \theta_k) \qquad (1)$$

where P is the transmitted signal power, T is the symbol duration, ω_c is the angular frequency of carrier, θ_k is the transmitted phase taken from one of M -phases $\{\frac{2\pi}{M}i,\ i=0,\ 1,\ \cdots\ M-1\}$ and p(t) represents pulse shaping and unity over each symbol duration.

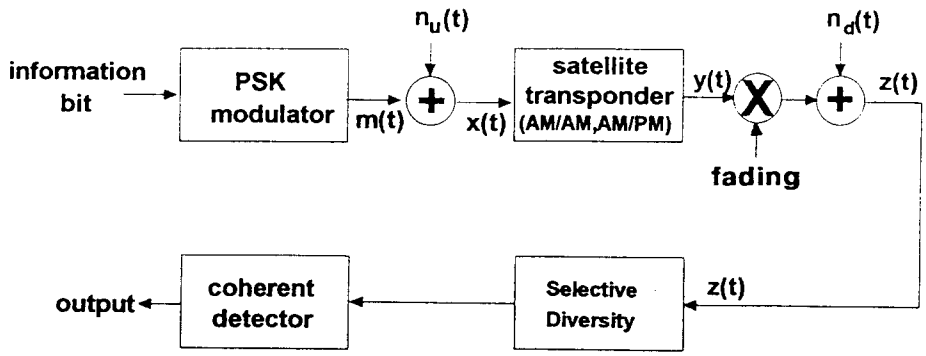

[Fig. 1] System model for PSK mobile satellite communication.

We assume θ_k, the phases of the transmitted signal, to be equally likely. Supposing that the front end filter at the satellite repeater is transparent, we can express the uplink signal as

$$x(t) = m(t) + n_u(t) \tag{2}$$

$$n_u(t) = n_{uc}(t)\cos\omega_c t - n_{us}(t)\sin\omega_c t \tag{3}$$

In Eq(3), $n_u(t)$ is a narrowband Gaussian noise and $n_{uc}(t)$, $n_{us}(t)$ are baseband Gaussian process. Since the uplink noise is a narrowband Gaussian process, the envelope R and the phase η of signal in uplink path is identical with the case of a sine wave plus a narrowband Gaussian process as given in ref.[3]

$$x(t) = R(t)\cos(\omega_c t + \theta_0 + \eta(t)) \tag{4}$$

The joint pdf (probability density function) of R and η is given in ref.[12]

$$P_u(R, \eta) = \frac{R}{2\pi\sigma_u^2} \cdot \exp\left[-\frac{R^2 + 2p - 2\sqrt{2p}R\cos\eta}{2\sigma_u^2}\right] \tag{5}$$

The output signal of the transponder is expressed as[3]

$$y(t) = f(R)\cos(\omega_c t + \theta_0 + \eta(t) + g(R)) \tag{6}$$

where f(R) represents the AM/AM conversion and g(R) AM/PM conversion at the satellite transponder. These two functions characterize the memoryless bandpass nonlinearity.

The transponder output y(t) is attenuated and faded in the downlink path. The envelope of attenuated and faded signal becomes F(R). We assume the slow fading with a normalized amplitude $\rho(=\sqrt{\frac{F(R)^2}{\overline{F(R)}^2}})$ which is Rician distributed[13], then the pdf of ρ is given by

$$p(\rho) = 2\rho(1+K)\exp[-K-\rho^2(1+K)] \cdot I_0(2\rho\sqrt{(1+K)}); \quad \rho \geq 0 \tag{7}$$

where the parameter K is the power ratio of coherent (line-of-sight) component to noncoherent (diffuse) component. Rayleigh fading is a special case of the Rician fading model and is corresponding to K=0 which characterizes terrestrial mobile radio channel.

Expressing again the Eq.[7] with $\rho = \sqrt{\frac{\gamma_k}{\gamma_{0k}}}$ (γ_k; instantaneous downlink CNR_d, γ_{0k}; average CNR_d),

$$p(\gamma_k) = \frac{(1+K)}{\gamma_{0k}} \exp[-K - \frac{\gamma_k}{\gamma_{0k}}(1+K)] \cdot I_0[2\sqrt{\frac{\gamma_k(K+K^2)}{\gamma_{0k}}}] \quad (8)$$

Assuming that the received signal corrupted by the Rician fading in each diversity branch are uncorrelated, we drived the pdf of the output instantaneous signal to noise ratio, $p(\gamma)$, at the M-branch SC diversity reception circuit as based on the procedure given in the reference[10]. Let γ be the maximum CNR, and its pdf $p(\gamma)$ can be expressed as

$$p(\gamma) = M(1 - Q(\sqrt{2K}, \sqrt{\frac{2(1+K)\gamma}{\gamma_0}}))^{M-1} \cdot \frac{(1+K)}{\gamma_0} \exp[-K - \frac{\gamma_k}{\gamma_{0k}}(1+K)] \cdot I_0[2\sqrt{\frac{\gamma(K+K^2)}{\gamma_0}}] \quad (9)$$

where γ_0 is the average CNR per symbol on each diversity reception.

In Eq. (9), we can see that the pdf $p(\gamma)$ is the same as Rician pdf in case of one branch ($M=1$).

And then the transponder output signal $y(t)$ is mixed with Gaussian noise $n_d(t)$ with zero mean and power spectral density $N_0/2$. We assume a conventional demodulator which includes a receiver filter, a sampler taking samples at an optimum instant on the quadrature and inphase channels. It is assumed that the carrier tracking loop will provide the mean phase $\bar{g}$ of the phase randomness due to AM/PM distortion. The decision device shall determine the transmitted phase based on the observation of the sample which can be expressed as

$$r = z + n_{dc} \quad (10)$$

$$\bar{r} = \bar{z} + n_{ds} \quad (11)$$

where,

$$z = F(R_0)\cos(\theta_0 + \eta_0 + g(R_0) - \bar{g}) \quad (12)$$

$$\bar{z} = F(R_0)\sin(\theta_0 + \eta_0 + g(R_0) - \bar{g}) \quad (13)$$

R_0 and η_0 represent the envelope R and phase η sampled at $t=t_0$ The pair $(r, \bar{r})$ is processed by the signal detector to determine which one of M phases, θ_0, was transmitted according to the phase decision zone in which $(r, \bar{r})$ lies as shown in [Fig. 2].

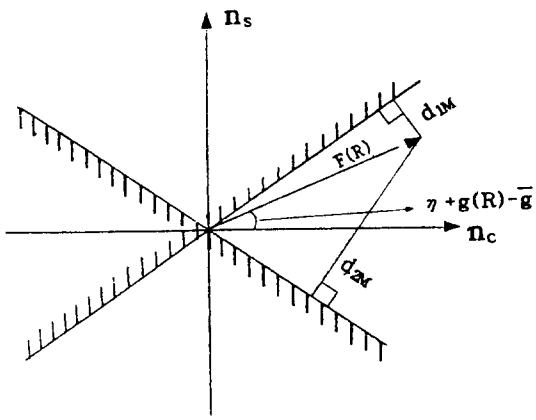

[Fig. 2] Decision zone for detecting transmitted phase.

In this mobile-satellite system, the TWT amplifier is typically characterized for AM/AM and AM/PM as follows[11]

$$f(R) = \alpha_a R/(1+\beta_a R^2) \quad (14)$$

$$g(R) = \alpha_b R^2/(1+\beta_b R^2) \quad (15)$$

where,

$\alpha_a = 1.9638$, $\beta_a = 0.9945$

$\alpha_b = 2.5293$, $\beta_b = 2.8168$

The transfer function of the above typical TWT amplifier is shown in [Fig. 3].

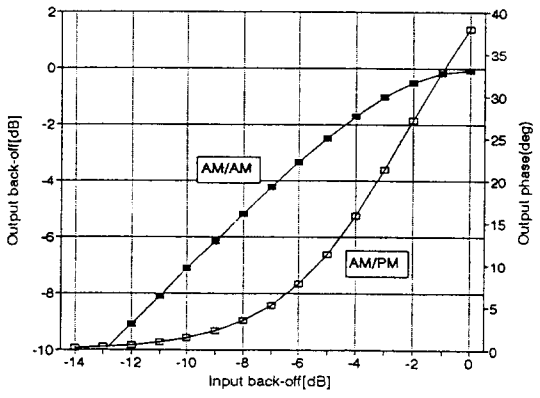

[Fig. 3] Transfer characteristic of TWTA.

Ⅲ. Conditional Error Rate

Without loss generality, we assume that the transmitted phase is zero, i.e., $\theta_0 = 0^0$. The receiver bases its decision on the pair (r, $\bar{r}$) where an error occurs if and only if (r, $\bar{r}$) falls outside of the decision zone of $\frac{2\pi}{M}$ radian centered at $\theta_0 = 0^0$. Then, the conditional average error rate may be expressed as[6, 7]

$$P_e(n_{dc}, n_{ds}, | R, \eta, \gamma) = \frac{1}{2}\,\mathrm{erfc}\left[\frac{z}{\sqrt{2}\sigma_d}\right] \text{ for BPSK}$$

$$P_e(n_{dc}, n_{ds}, | R, \eta, \gamma) = \frac{1}{2}\,\mathrm{erfc}\left[\frac{d_{1M}}{\sqrt{2}\sigma_d}\right] + \frac{1}{2}\,\mathrm{erfc}\left[\frac{d_{2M}}{\sqrt{2}\sigma_d}\right] - \frac{1}{4}\,\mathrm{erfc}\left[\frac{d_{1M}}{\sqrt{2}\sigma_d}\right]\mathrm{erfc}\left[\frac{d_{2M}}{\sqrt{2}\sigma_d}\right] \quad (16)$$

for QPSK

where,

$$z = F(R)\cos(\eta + (g(R) - \bar{g})) \quad (17\text{-a})$$

$$d_{1M} = F(R)\sin(\frac{\pi}{4} - \eta - (g(R) - \bar{g}) \quad (17\text{-b})$$

$$d_{2M} = F(R)\sin(\frac{\pi}{4} - \eta - (g(R) - \bar{g}) \quad (17\text{-c})$$

For convenience, we dropped the subscript '0' for all R.

Ⅳ. Average Error Rate

The conditional error rate $P_e(n_{dc}, n_{dc}|R, \eta, \gamma)$ should be averaged over the statistics of R, η which are functions of the uplink noise and γ of the selector output CNR.

Thus, the average error rate is represented by

$$P_E = \int_0^{\infty}\int_0^{2\pi}\int_0^{\infty} P_e(n_{dc}, n_{ds}|R, \eta, \gamma) \cdot P_u(R, \eta)\, p(\gamma) dR\, d\eta\, d\gamma \quad (18)$$

In order to find the more exact average error rate and simplify the calculation, the standard Gauss quadrature rule to carry out the expectation over R is used as

$$P_u(R, \eta) = \frac{R}{2\pi\sigma_u^2}\exp\left[-\frac{R^2 + 2p - 2\sqrt{2p}R\cos\eta}{2\sigma_u^2}\right] = \frac{R}{2\pi\sigma_u^2}\exp\left[-\frac{P}{\sigma_u^2}\sin^2\eta\right] \cdot \exp\left[-\frac{(R + \sqrt{2p}\cos\eta)^2}{2\sigma_u^2}\right] \quad (19)$$

In the Eq.(19), for convenience, define a variable

$$x = \frac{R - \sqrt{2p}\cos\eta}{\sqrt{2}\sigma_u} \quad (20)$$

Thus the Eq.(18) can be expressed as follows:

$$P_E = \int_0^{\infty}\int_0^{2\pi}\int_0^{\infty} h(R', \eta)\, p_1(R', \eta) \cdot p(\gamma)\, e^{-x^2}\, dx\, d\eta\, d\gamma \quad (21)$$

where,

$$p_1(R', \eta) = \frac{R'}{\sqrt{2\pi}\sigma_u}\exp\left[-\frac{P}{\sigma_u^2}\sin^2\eta\right]$$

$$h(R', \eta) = P_e(n_{dc}, n_{ds}|R', \eta, \gamma)$$

$$R' = \sqrt{2}(\sigma_u x + \sqrt{P}\cos\eta)$$

$$a = -\frac{\sqrt{P}}{\sigma_u}\cos\eta$$

Here the SC diversity pdf of the random variable γ can be expressed as Eq. (9).

Then, the Nth moment of γ is represented by

$$\mu_n = \int_0^\infty \gamma^n p(\gamma)d\gamma \tag{22}$$

From Eqs. (9) and (22), we can show that (see Appendix A)

$$\mu_n = CM\left(\frac{1}{4b}\right)^n \left(\frac{1}{2b}\right)\exp[-K(M-1)] \cdot \left\{\sum_{\ell=1}^{\infty}\left(\frac{1}{2K}\right)^{\ell}\sum_{i=0}^{\infty}\left(\frac{\frac{1}{2}^{2i+\ell}}{i!\Gamma(\ell+i+1)}\right)\right\}^{M-1} \cdot \sum_{m=0}^{\infty}\frac{\frac{1}{2}}{m!\Gamma(m+1)} \cdot \frac{\{\ell(M-1+i(M-1)+m+n\}!}{2\left(\frac{aM}{4b}\right)^{\ell(M-1)+i(M-1)+m+n+1}} \tag{23}$$

where,

$a = (1+K)/\gamma_0$,
$b = (K^2+K)/\gamma_0$,
$c = (1+K)e^{-K}/\gamma_0$

The approximate discrete probability distribution γ_ℓ, $\omega_\ell(\ell = 1, 2, \cdots, v)$ for the random variable γ is required to satisfy the moment constraints

$$\mu_K = \sum_{\ell=1}^{v}\omega_\ell \gamma_\ell^K \tag{24}$$

The above discrete probability distribution γ_ℓ, ω_ℓ is obtained by the Classical Moment Technique (see Appendix B).

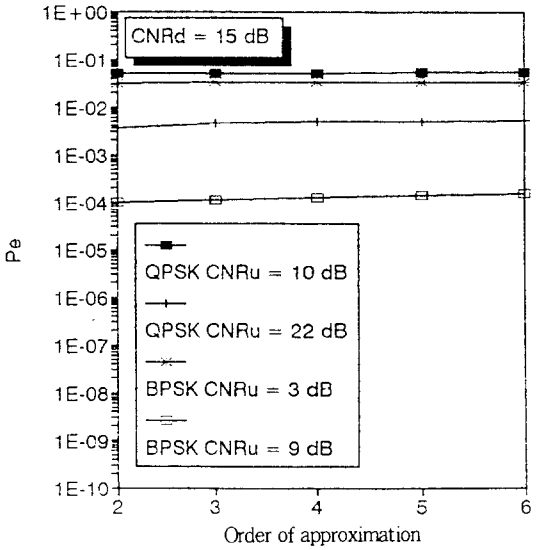

[Fig. 4] Accuracy of the classical moment applied to the performance evaluation of BPSK and QPSK signals.

In general, as the order of approximation is increased, we can obtain the more accurate performance. In this paper, we have found that only a relatively low order of approximation ($v \le 6$) is needed for the Rician distribution (M = 1 in the pdf of SC diversity) since the numerical results approach the same quantity as the order of approximation is increased, and it is well shown in [Fig. 4].

Then by the Gauss Quadrature Rule and the Classical Moment Technique for obtaining the approximate discrete probability density γ_ℓ, ω_ℓ for the above $p(\gamma)$, P_E can be expressed as

$$P_E = \sum_{\ell}\sum_{n}\sum_{m}\omega_\ell C_n C_m h(x_m, \eta_n, \gamma_\ell)p_1(x_m, \eta_n) \cdot u(x_m + \frac{\sqrt{P}}{\sigma_u}\cos\eta_n) \tag{25}$$

where,

$$u(\cdot) = \begin{cases} 1, & \ge 0 \\ 0, & < 0 \end{cases}$$

(C_m, x_m) = Gauss-Hermite quadrature parameters given in ref.(8)

(C_n, η_n) = Weight factors for Gaussian integration given in ref.(8)

(ω_ℓ, γ_ℓ) = Weight parameters obtained by Classical Moment Technique

We hereby define the downlink transmission power P_d as the output power of nonlinearity in the absence of uplink channel noise. The downlink $CNR_d(=\gamma_k)$ is then defined as $P_{d/\sigma d}{}^2$

V. Numerical Results

The numerical results given here are for BPSK and QPSK signals with fading factor K, using the numerical technique presented in the previous section. The characteristics of the TWT amplifier for this paper are shown by the set of curves given in [Fig. 3], and the input back-off for evaluating the numerical results is 2.5[dB] (see [Fig. 3]). In order to demonstrate the convergence of the numerical results with respect to the order of approximation used for the Rician distribution (M = 1 in the pdf of SC diversity), [Fig. 4] shows the error performance of BPSK and QPSK signals in the same environment.

With reference from [Fig. 5] to [Fig. 8], the error performances of BPSK and QPSK signals with Rician fading (M = 1 in Eq.(23)) are shown, and with reference from [Fig. 9] to [Fig. 12], the error performances of BPSK and QPSK siganls are shown when two-branch SC diversity (M = 2 in Eq.(23)) is adopted.

From the results of [Fig. 5] ~ [Fig. 14], it is obvious that uplink noise parameter has a serious effect on the system performance, and particularly the case accompanying the fading on the downlink has more serious effect. And also we can see that for a fixed fading factor K the curves of error performance converge to constant values at low uplink and downlink CNR's.

And finally from [Fig. 9] to [Fig. 14], we can see that the error performance degraded by fading can be mostly compensated by diversity reception.

VI. Conclusion

This paper provides an overall performance analysis to optimize the design of the BPSK and QPSK modulation schemes including the uplink noise parameter as well as nonlinear TWT amplifier in addition to the downlink fading effect presented in the conventional analyses on mobile-satellite communication. To make possible the performance evaluation having numerical complexity, the discrete probability values of the Rician pdf are firstly obtained by using the Classical Moment Technique. The accuracy if introducing the discrete values in evaluating the performance is confirmed graphically in this paper. Therefore, it is shown that it is sufficiently accurate to be used as a method for design of the system to reduce the degradation in the performance of mobile-satellite channel considering nonlinearity in TWT amplifier.

The results of numerical evaluation are given for a fixed fading factor. It is shown that (1) the uplink noise parameter has a serious effect on the system performance, (2) particularly the case accompanying the fading on the downlink has more serious effect, (3) for a fixed fading the curves of error performance converge to constant values at low uplink and downlink CNR's, and (4) the error performance degraded by fading can be mostly compensated for by diversity reception.

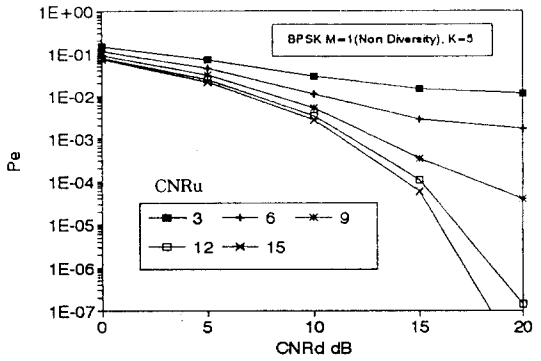

〔Fig. 5〕 Performance of BPSK signal with fading (K = 5).

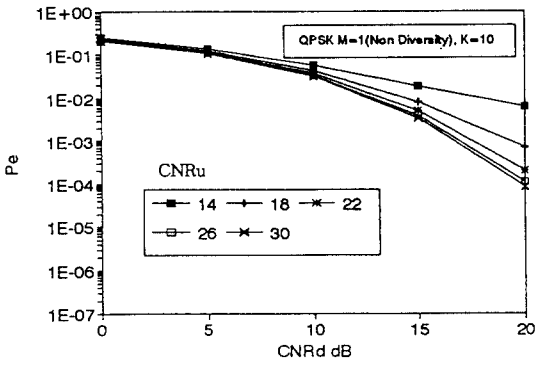

〔Fig. 8〕 Performance of QPSK signal with fading (K = 10).

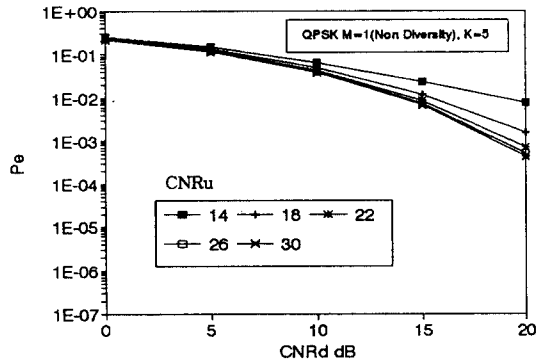

〔Fig. 6〕 Performance of QPSK signal with fading (K = 5).

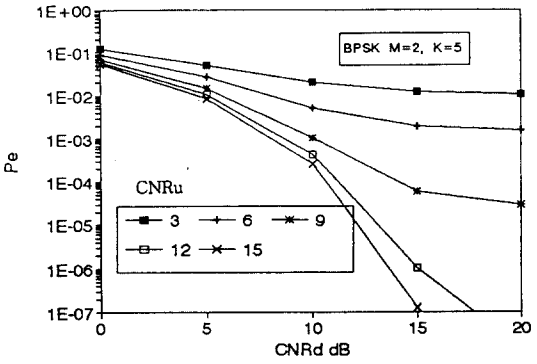

〔Fig. 9〕 Performance of BPSK signal with SC diversity (K = 5).

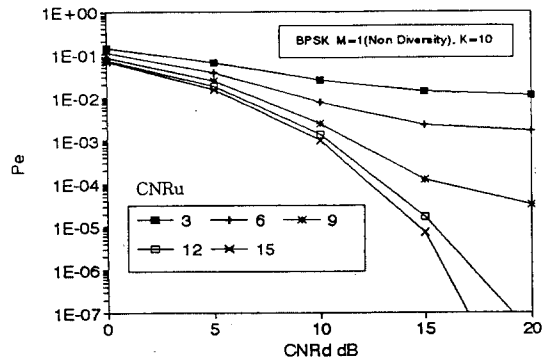

〔Fig. 7〕 Performance of BPSK signal with fading (K = 10).

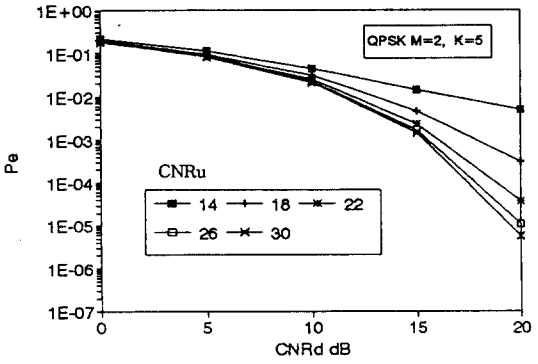

〔Fig. 10〕 Performance of QPSK signal with SC diversity (K = 5).

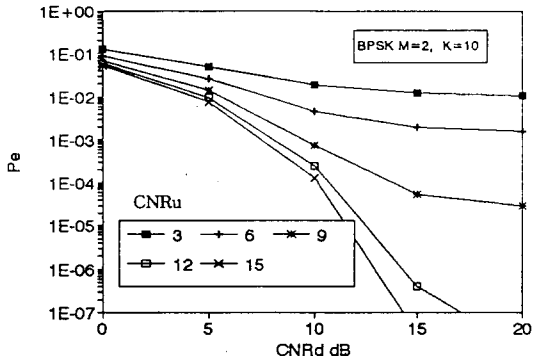

[Fig. 11] Performance of BPSK signal with SC diversity (K = 10).

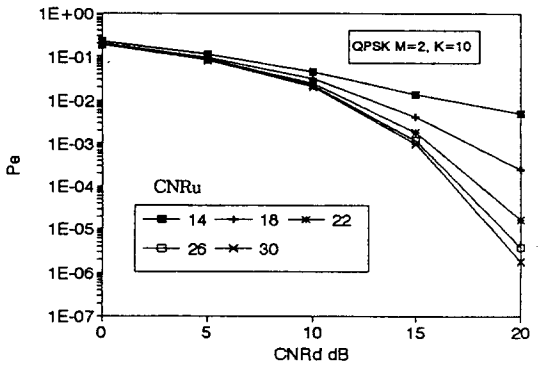

[Fig. 12] Performance of QPSK signal with SC diversity (K = 10).

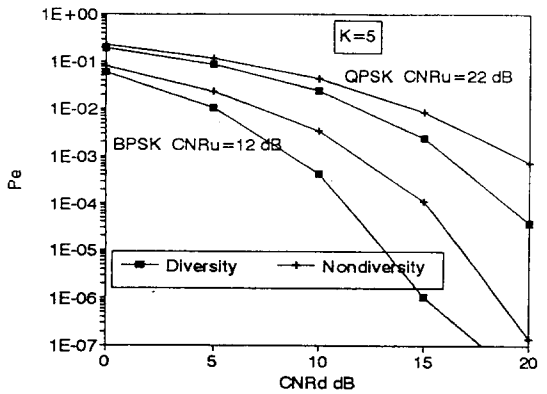

[Fig. 13] Comparison of BPSK and QPSK signals with fading and SC diversity (K = 5).

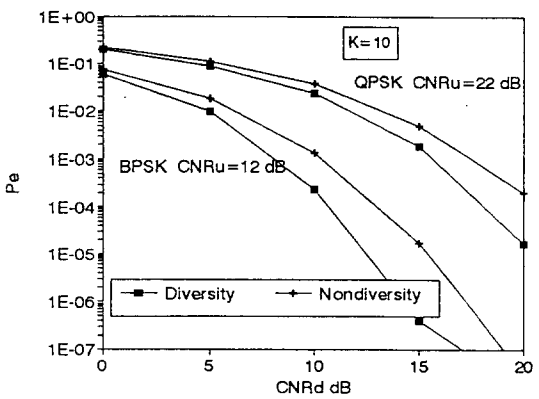

[Fig. 14] Comparison of BPSK and QPSK signals with fading and SC diversity (K = 10).

Appendix A

〈Derivation of Eq.(23)〉

$$\mu_n = \int_0^\infty \gamma^n \cdot M\left\{1 - Q\left(\sqrt{2K}, \sqrt{\frac{2\gamma(1+K)}{\gamma_0}}\right)\right\}^{M-1} \cdot \frac{1+K}{\gamma_0} \exp\left(-\frac{\gamma(1+K)}{\gamma_0} - K\right) I_0\left(2\sqrt{\frac{K\gamma(1+K)}{\gamma_0}}\right) d\gamma \qquad (A.1)$$

Using the formulas[9, 10, 16]

$$I_\nu(z) = \sum_{m=0}^{\infty} \frac{\left(\frac{1}{2}z\right)^{\nu+2m}}{m!\Gamma(\nu+m+1)}$$

and $$Q(x, y) = 1 - \exp\left(-\frac{x^2+y^2}{2}\right) \sum_{\ell=1}^{\infty} \left(\frac{y}{x}\right)^\ell I_\ell(xy) \qquad (A.2)$$

We can obtain μ_n as follows:

$$\mu_n = \int_0^\infty \gamma^n \cdot M\left\{\exp\left(-\frac{2K + \frac{2\gamma(1+K)}{\gamma_0}}{2}\right)\right.$$

$$\sum_{\ell=1}^{\infty}\left(\frac{\gamma(1+K)}{K\gamma_0}\right)^{\ell}\cdot\left\{I_{\ell}\left(2\sqrt{\frac{K\gamma(1+K)}{\gamma_0}}\right)\right\}^{M-1}\cdot\frac{1+K}{\gamma_0}\cdot\exp\left(-\frac{\gamma(1+K)}{\gamma_0}-K\right)I_0\left(2\sqrt{\frac{K\gamma(1+K)}{\gamma_0}}\right)d\gamma$$

$$=CM\left(\frac{1}{4b}\right)^{n}\left(\frac{1}{2b}\right)\exp[-K(M-1)]\cdot\left\{\sum_{\ell=1}^{\infty}\left(\frac{1}{2K}\right)^{\ell}\sum_{i=1}^{\infty}\left(\frac{\left(\frac{1}{2}\right)^{2i+\ell}}{i!\Gamma(\ell+i+1)}\right)\right\}^{M-1}\cdot\sum_{m=0}^{\infty}\frac{\left(\frac{1}{2}\right)^{2m}}{m!\Gamma(m+1)}\cdot\frac{\{\ell(M-1)+i(M-1)+m+m\}!}{2\left(\frac{aM}{4b}\right)^{\ell(M-1)+i(M-1)+m+m+1}} \quad (23)$$

where $a=\frac{1+K}{\gamma_0}$, $b=\frac{K(1+K)}{\gamma_0}$,

$C=\frac{(1+K)e^{-K}}{\gamma_0}$

Appendix B

〈A Construction Method for CMT〉

We present an algorithm to construct the approximate discrete proability distribution γ_ℓ, ω_ℓ ($\ell=1,2,\cdots v$)for a random variable γ where only moments μ_K, K=0,1,2,⋯ are known. This approximate probability distribution is required to satisfy the moment constraints

$$\mu_k=\sum_{\ell=1}^{v}\gamma_\ell\,\omega_\ell{}^K \text{ for } K\le n \quad (B.1)$$

We set N=2v−1 and define two polynomials

$$g(Z)=\sum_{K=0}^{N}\mu_K Z^K \quad (B.2)$$

$$h(Z)=\sum_{K=0}^{N}\mu_{N+1+K}Z^K \quad (B.3)$$

where μ_{N+1+K}, $K=0,1,2,\cdots$ are extended moments defined by

$$\mu_k=\sum_{\ell=1}^{v}\gamma_\ell\,\omega_\ell{}^K \text{ for } K\le N+1,\ N+2,\ \cdots \quad (B.4)$$

One can show that the polynomial

$$\mu(Z)=\sum_{K=0}^{\infty}\mu_K Z^K=g(Z)+Z^{N+1}h(Z) \quad (B.5)$$

or

$$=\sum_{\ell=1}^{v}\frac{\omega_\ell}{1-\gamma_\ell Z} \quad (B.6)$$

Let $\sigma(Z)=\Pi_{\ell=1}^{v}(1-\gamma_\ell\cdot Z)$ where the degree of the $\sigma(Z)$ is less than or equal to v. Then, one has

$$g(Z)\,\sigma(Z)+Z^{N+1}h(Z)\,\sigma(Z)=\eta(Z) \quad (B.7)$$

where

$$\eta(Z)=\sum_{\ell=1}^{v}\omega_\ell\,\Pi_{\ell'\neq\ell}(1-\gamma_{\ell'}\cdot Z) \quad (B.8)$$

Since the second term is of no concern, as will become clear later, we shall utilize the approach of the Euclid decoding algorithm to obtain $\sigma(Z)$ and $\eta(Z)$. First, start with two initial polynomials $\gamma_{-1}(Z)=Z^{N+1}$ and $\gamma_0(Z)=g(Z)$.

The Euclid algorithm is performed on $\gamma_{-1}(Z)$ and $\gamma_0(Z)$ until the degree of the h_{th} remainder $\gamma_h(Z)$ is less than v.

$$\gamma_{-1}(Z)=q_1(Z)\,\gamma_0(Z)+\gamma_1(Z) \text{ deg } \gamma_0>\text{deg } \gamma_1 \quad (B.9)$$

$$\gamma_0(Z)=q_2(Z)\,\gamma_1(Z)+\gamma_2(Z) \text{ deg } \gamma_1>\text{deg } \gamma_2 \quad (B.10)$$

:

:

$$\gamma_{i-2}(Z) = q_i(Z)\,\gamma_{i-1}(Z) + \gamma_i(Z) \quad \deg\gamma_{i-1} > \deg\gamma_i \tag{B.11}$$

where $q_i(Z)$ is a quotient polynomial and $\gamma_i(Z)$ is the i_{th} remainder polynomial The above relation can be put in a matrix form

$$\begin{bmatrix}\gamma_{i-2}(Z)\\ \gamma_{i-1}(Z)\end{bmatrix} = Q_i(Z)\begin{bmatrix}\gamma_{i-1}(Z)\\ \gamma_i(Z)\end{bmatrix} \tag{B.12}$$

where

$$Q_i(Z) = \begin{bmatrix} q_i(Z) & 1\\ 1 & 0\end{bmatrix} \tag{B.13}$$

From Eq.(B.12), we obtain

$$\begin{bmatrix}\gamma_{i-2}(Z)\\ \gamma_0(Z)\end{bmatrix} = Q(Z)\begin{bmatrix}\gamma_{i-1}(Z)\\ \gamma_i(Z)\end{bmatrix} \tag{B.14}$$

where

$$\begin{aligned} Q(Z) &= Q_1(Z)\,Q_2(Z)\cdots Q_i(Z)\\ &\equiv \begin{bmatrix} U_i(Z) & U_{i-1}(Z)\\ V_i(Z) & V_{i-1}(Z)\end{bmatrix}\end{aligned} \tag{B.15}$$

Note that $U_i(Z)$ and $V_i(Z)$ are functions of $q_i(Z)$. One can show that the matrix $Q(Z)$ is nonsingular and its determinant is equal to $(-1)^i$. Therefore, one has

$$\begin{bmatrix}\gamma_{i-1}(Z)\\ \gamma_i(Z)\end{bmatrix} = (-1)^i\begin{bmatrix} V_{i-1}(Z) & -U_{i-1}(Z)\\ -V_i(Z) & U_i(Z)\end{bmatrix}\begin{bmatrix}\gamma_{i-1}(Z)\\ \gamma_0(Z)\end{bmatrix} \tag{B.16}$$

From this results, we have for h_{th} division

$$U_h(Z)g(Z) - Z^{N+1}V_h(Z) = (-1)^h\gamma_h(Z) \tag{B.17}$$

Comparing Eq.(B.7) and Eq.(B.17), we identify that

$$\sigma(Z) = \frac{1}{C_0}U_h(Z) \tag{B.18}$$

and

$$\eta(Z) = \frac{1}{C_0}(-1)^h\gamma_h(Z) \tag{B.19}$$

where C_0 is the constant term of the polynomial $U_h(Z)$.

The roots of $U_h(Z)$ give γ_1^{-1}, γ_2^{-1},…, γ_ν^{-1} whose weights can be obtained from Eq.(B.19)

$$\omega_\ell = \frac{1}{C_0}\left(\frac{(-1)^h\gamma_h(\gamma_L^{-1})}{\Pi_{\ell'\neq\ell}(1-\gamma_{\ell'}\cdot\gamma_\ell^{-1})}\right) \tag{B.20}$$

Since the long division is easy to perform, the method of finding the weights ω_ℓ appears to be considerably simpler than other schemes which essentially require solving Eq.(B.1) for $(\gamma_\ell, \omega_\ell)$

References

1. W. C. Y. Lee, *Mobile Communications Design Fundamentals*, Howard W. Sams & Co., 1986.
2. F. Davarian, "Fade margin calculation for channels impaired by Rician fading", IEEE Trans. on Vehicular Technology, vol. VT-34, no. 1, Feb. 1985.
3. T. C. Huang, J. K. Omura, and W. C. Lindsey, "Analysis of cochannel interference and noise", IEEE Trans. on Commun., vol. COM-29, pp. 593~604, May 1981.
4. I. K. Hwang and L. Kurz, "Digital data transmission over nonlinear satellite channels with interference, cochannel interference and noise", Dissertation at the Polytechnic University, March 1990.
5. P. Hetrakul and D. P. Taylor, "The effects of transponder nonlinearity on binary CPSK signal

transmission", IEEE Trans. on Commun., pp. 546-553, May 1976.

6. V. K. Prabhu, "Error rate consideration for coherent phase shift keyed systems with cochannel interference", Bell System Technical Jounal, vol.48, pp.743~767, March 1969.
7. A. S. Rosenbaum, "Binary PSK error probabilities with multiple cochannel interferences", IEEE Trans. on Commun., vol. COM-15, no.3, June 1970.
8. M. Abramowitz and I. A. Stegum, "Handbook of mathematical functions", National Bureau of Standards, Washington, D.C.., Dec. 1972.
9. I. S. Gradshteyn and I. M. Ryzhik, *Table of Integrals, Series and Products,* Academic Press, New York, 1965.
10. M. Schwartz, W. R. Bennett and S. Stein, *Communication Systems and Techniques,* New York; McGraw-Hill, 1966.
11. A. A. M. Saleh, "Frequency-independent and frequency-dependent nonlinear models of TWT amplifiers", IEEE Trans. on Commun., vol. COM-29, no.11, Nov.1981.
12. A. D. Whalen, *Detection of Signals in Noise.* Academic Press, 1971.
13. D. Divsalar, M. K. Simon, T. Jedrey, N. Lay and W. Rafferty, "Combined trellis coding and feedforward processing for MSS applications", International Mobile Satellite Conference, pp. 175-181, June 1990.
14. C. Loo, "A statistical model for a land mobile satellite link", IEEE Trans. on Vehicular Technology, vol.VT-34, no.3, Aug. 1985.
15. Y. Karasawa and M. Yasunaga, "Interference evaluation method for mobile- satellite systems under Nakagami-Rice fading conditions", IEICE Trans., Commun., vol. E75-B, no.1, Jan. 1992.
16. W. Magnus, *Formulas and theorems for the Special Functions of Mathematical Physics.* Springer-Verlag in Germany, 1966.